INTERACTION BETWEEN TWO FLAT CHARGES EXPLODING ON THE GROUND

N. B. Il'inskii and N. D. Yakimov

UDC 534.222.2;622.235.5

A study has been made [1] of the hydrodynamic interaction between two point charges exploded on the surface of the ground; it was assumed there that Lavrent'ev's solid–liquid model may apply within the yield region, which implies zones having velocities below the critical value, which implies that there is a range in L (where 2L is the distance between the charges) in which the solution is not unique. In this study of interaction between charges it is also assumed, as in [2], that there is a zone at rest in the soil, as in the case of a symmetrical charge of variable cross section. This zone at rest allows one to retain the solid–liquid model while obtaining a unique solution of one sheet.

We consider the boundary to the crater produced by two identical flat charges placed on the surface of the ground; the solid–liquid model is used, in which the motion is described by the equation for an ideal incompressible liquid for all points where the speed is $v > v_*$ (v_* is the critical speed). Outside the zone where $v > v_*$, the soil is taken as absolutely solid. The boundary between the two regions is a solid wall and is defined from the condition $v = v_*$. Figure 1 shows the corresponding model for the general case, where AB and A'B' are the flat charges, CQC' is the free surface, CDC' is the boundary of the crater, and HNH'M is the immobile area, i.e., an absolutely solid part where $v = v_*$ at the boundary (as at the edge of the crater).

By virtue of the symmetry with respect to the y axis, we need consider only the right-hand half of the motion, which is denoted by G_z, while the boundary is denoted by Γ_z. The initial parameters are the following: the width l of the charge AB, the velocity potential φ_0 there, the critical velocity v_*, and the distance 2L between the charges (L = QA). If we introduce the following dimensionless relations:

$$w' = w/\varphi_0,\ v' = v/v_*,\ z' = zv_*/\varphi_0,$$

where $z = x + iy$ is the physical plane and $w = \varphi + i\psi$ is the complex flow potential, then the solution is dependent only on the parameters $l' = lv_*/\varphi_0$ and $L' = Lv_*/\varphi_0$, since $\varphi_0' = 1$, $v_*' = 1$; in what follows we utilize the dimensionless variables while omitting the primes for simplicity.

The problem is reducible to the following boundary-value problem: determine the position and shape of the unknown parts CD and MHN on the boundary Γ_z such that a function analytical in G_z and continuous in $\overline{G}_z$ (apart from the points A and B) is to be found as $w(z) = \varphi(x, y) + i\psi(x, y)$ to satisfy the following conditions on Γ_z:

$$\varphi = -1 \text{ on } AB;\ \varphi = 0 \text{ on } QA, BC;\ \psi = 0 \text{ on } QNHMDC; \quad (1)$$

$$\partial\varphi/\partial s = -1 \text{ on } NH;\ \partial\varphi/\partial s = 1 \text{ on } HM, DC, \quad (2)$$

where s is the abscissa of a point on Γ_z reckoned along the curve. Function w(z) should have logarithmic singularities at A and B.

In the plane of the variable $w = \varphi + i\psi$, the solution should correspond to region G_w on the basis of condition (1), while in the plane of the variable $\omega = dw/dz = v_x - iv_y$ it should correspond to G_ω by virtue of condition (2), as in Fig. 2, where the corresponding points in the different planes are denoted by the same letters. So far the positions of the vertices have not been determined for these regions. Further, we also do not know the positions of the points M, N, and D on the boundary of G_w, nor do we know the positions of points H and Q on the boundary of G_ω.

Kazan'. Translated from Zhurnal Prikladnoi Mekhaniki i Tekhnicheskoi Fiziki, No. 1, pp. 147-151, January-February, 1977. Original article submitted March 2, 1976.

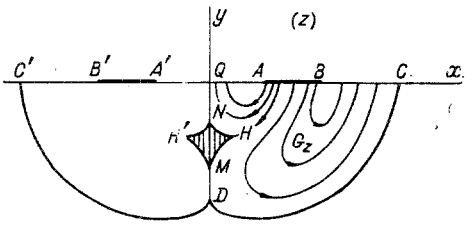

Fig. 1

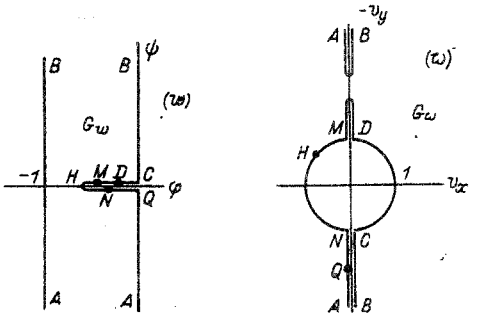

Fig. 2

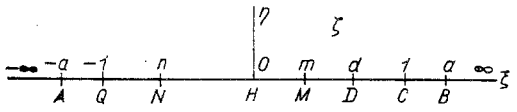

Fig. 3

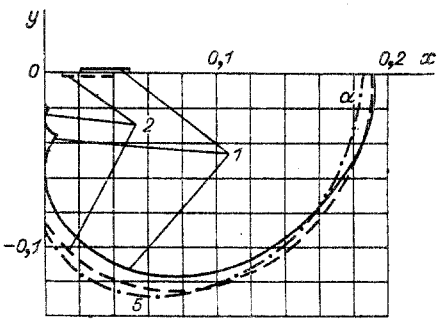

Fig. 4

We introduce the auxiliary half-plane Im $\zeta > 0$ (denoted by G_ζ) of the variable $\zeta = \xi + i\eta$ (Fig. 3) in order to construct the solution; then we map G_w and G_ω conformally onto G_ζ to find the solution as the function that maps G_ζ on G_z:

$$z(\zeta) = \int_{-1}^{\zeta} \frac{w'(\zeta)}{\omega(\zeta)}\, d\zeta. \tag{3}$$

The derivative $w'(\zeta)$ for the mapping of G_ζ on G_w is given by the Christoffel–Schwarz formula as follows on the basis of the symmetry of the regions:

$$w'(\zeta) = \zeta K/(\zeta^2 - a^2)\sqrt{\zeta^2 - 1}, \tag{4}$$

where $K = -(2i/\pi)\sqrt{a^2 - 1}$.

The function $\omega(\zeta)$ that maps G_ζ on G_ω is represented as a superposition of the three functions $\omega\{\zeta_2[\zeta_1(\zeta)]\}$ in accordance with the formulas

$$\zeta_1 = \frac{(1+k)\zeta - 1 + k}{(n+k)\zeta - n + k}, \quad \zeta_2 = 1 - \frac{2\left(d_1^2 - a_1^2\right)\left(\zeta_1^2 - 1\right)}{\left(d_1^2 - 1\right)\left(\zeta_1^2 - a_1^2\right)},$$
$$\omega = -i\left(\zeta_2 + \sqrt{\zeta_2^2 - 1}\right), \tag{5}$$

where $a_1 = \zeta_1(a)$; $d_1 = \zeta_1(d)$; $k = \sqrt{(a^2 - n^2)/(a^2 - 1)}$.

The symmetry of G_ω and the symmetry of the corresponding region in the plane of ζ_1 gives us

$$m = [(a^2 + n)d - a^2(n + 1)]/[(n + 1)d - a^2 - n]. \tag{6}$$

The other parameters a, n, and d appearing in (4) and (5) are found from a system of three nonlinear equations for $w'(\zeta)$ and $\omega(\zeta)$:

$$\int_{-1}^{-a} \frac{w'(\zeta)}{\omega(\zeta)}\, d\zeta = L'; \tag{7}$$

$$\int_{-a}^{\infty} \frac{w'(\zeta)}{\omega(\zeta)}\, d\zeta - \int_{a}^{\infty} \frac{w'(\zeta)}{\omega(\zeta)}\, d\zeta = l'; \tag{8}$$

$$\int_{0}^{n} w'(\zeta)\,\mathrm{Re}\,\omega(\zeta)\, d\zeta - \int_{0}^{m} w'(\zeta)\,\mathrm{Re}\,\omega(\zeta)\, d\zeta = 0, \tag{9}$$

TABLE 1

Example	φ_0'	L'	l'	$-y_N$	x_H	$-y_H$	$-y_M$	$-y_D$	x_C
1	1	0,02	0,03	0,029	0,008	0,034	0,051	0,058	0,189
2	1	0,01	0,03	0,020	0,002	0,021	0,024	0,080	0,190
3	1	0,02	0,06	0,037	0,010	0,044	0,063	0,083	0,268
4	2	0,02	0,03	0,030	0,003	0,033	0,036	0,113	0,262
5	1	0	0,03	—	—	—	—	0,087	0,185
6	1	0	0,06	—	—	—	—	0,116	0,264

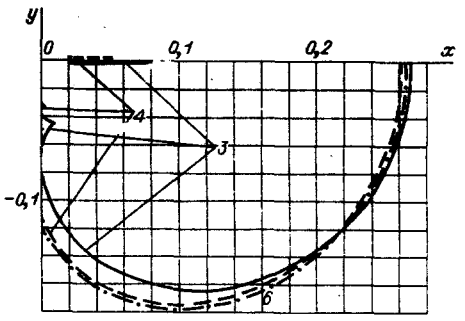

Fig. 5

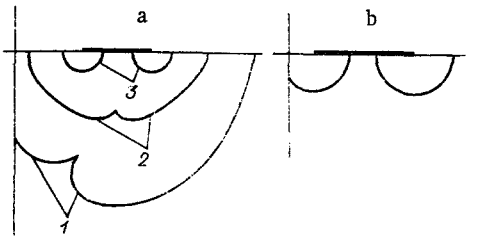

Fig. 6

which is derived from the conditions $z(-\alpha) = L'$, $z(\alpha) - z(-\alpha) = l'$ and the specification that MD lies on the line x = 0.

In numerical calculations, it is usually simpler to use a partly reversed formulation, in which two parameters are specified, for instance, α and d, whereupon the third parameter n is derived from (9). Then L' and l' are defined by (7) and (8). However, the resulting series of solutions in terms of two parameters is inconvenient for practical purposes, so it is better to take the direct approach presented above, i.e., specification of l' and L' and derivation of α, n, and d from (7)-(9). This is the formulation used below in the M-222 computer calculations. Figures 4 and 5 show the more interesting results.

In the examples, the input quantities L' and l' (Table 1) were selected to make the results comparable; for instance, example 2 was calculated with the distance between the charges smaller than that in example 1, but all the other conditions the same (Fig. 4). It is clear that reducing the distance causes the immobile area to rise toward the surface and become smaller, while the depth of the crater increases. For comparison, line 5 in Fig. 4 shows the boundary of the crater in the limiting case L' = 0, which corresponds to the solution of [3].

Example 3 differs from example 1 in that the charge width has been doubled, while in example 4 the charge weight has been doubled, i.e., $\varphi_0' = 2$ for the same distance L' between the charges (Fig. 5). Examples 3 and 4 differ in charge width but are the same in charge energy and separation. Example 4 differs from example 3 in that the depth of the crater has been increased while the area of the immobile region is less. Line 6 in Fig. 5 shows the crater for the charge of example 3 but with L' = 0. The coordinates of the characteristic points on the boundary are listed in Table 1.

The values of L' and l' show that the shape of the crater takes one of the forms shown in Fig. 6, apart from the instance of Fig. 1; for example, while the shape of Fig. 1 occurs for certain L' and l', any increase in L' or reduction in l' causes MD to fall to zero, and the solution takes the form of 1 (Fig. 6a) if there is any further change in L' or l'. If the variation in L' or l' is continued, the crater splits up into two independent areas, without interaction between the charges (form 2, Fig. 6a). If L' and l' are sufficiently large, there may be four such areas (form 3, Fig. 6a). If l' is large, there may be three unconnected areas, with charge interaction in the central region (Fig. 6b).

The case where G_z takes the form 1 of Fig. 6a is a particular case of the one examined in detail above: regions G_w and G_ω have the forms shown in Figs. 2 and 3 (points M and D are chosen appropriately), while there is no vertical section MD in G_ω. The solution can still be derived from (3), but one should put $d_1 = 0$ in (5). Equations (6) and (9) are no longer necessary, and we have merely (7) and (8) to determine α and n. Any attempt to define a

solution in this way for L' and l' such that there is a solution as in Fig. 1 results in a solution with more than one sheet (points at which x is less than 0 appear on curve HC).

The other cases, where the crater splits up into unconnected areas, are of little interest from the viewpoint of charge interaction and therefore are not considered.

LITERATURE CITED

1. V. M. Kuznetsov, É. B. Polyak, and E. N. Sher, "The hydrodynamic interaction of extended explosive charges," Zh. Prikl. Mekh. Tekh. Fiz., No. 5, 93-101 (1975).
2. N. B. Il'inskii, A. G. Labutkin, and R. B. Salimov, "A case of explosion of a symmetrical surface charge of variable thickness," Zh. Prikl. Mekh. Tekh. Fiz., No. 3, 154-161 (1976).
3. V. M. Kuznetsov, "The shape of the crater produced by an explosion on the surface of the ground," Zh. Prikl. Mekh. Tekh. Fiz., No. 3, 152-156 (1960).

SPALLING IN STEEL PRODUCED BY EXPLOSION OF A SHEET CHARGE AND COLLISION OF A PLATE

A. P. Rybakov

UDC 539.42:620.178

A specific type of damage (spalling) occurs in strong shock waves and in explosions acting on barriers composed of material of finite tensile strength. The tensile stresses that produce the spalling and fracture arise by interaction between colliding waves. Failure is then always preceded by compression in shock waves.

There are very many papers on such spalling, and one of the early extensive studies [1] gave a detailed description of the phenomena produced in metals by explosive loading. In particular, there was a fairly detailed description of spalling, with an attempt to measure a quantitative characteristic, namely, the critical stress. Subsequent studies [1-13] have provided quantitative criteria and schemes based on finite failure times [2], the dislocation mechanism of failure [12], and a quasiacoustic approximation in terms of stored elastic energy [13].

Shock loading can occur in various ways, e.g., detonation of a block of explosive in contact with an obstacle, collision of a plate, or detonation of a sheet of explosive. Two different situations occur, namely, a planar shock wave propagating into the obstacle or parallel to the free surface, the general case being propagation at some angle α. The critical failure stress may be determined from the difference between the initial speed w_0 of the free surface and the mean speed $\overline{w}$:

$$p_{cr} = (1/2)\rho_0 c_0 \Delta w, \quad (1)$$

where ρ_0 and c_0 are the density and speed of sound in the material. If the shock wave is incident at right angles $\Delta w = w_0 - \overline{w}$ [2], while a shock wave emergent at an angle to the surface gives $\Delta w = w_0 - \overline{w}/\cos\alpha$ [7, 8].

We have examined the effects of sheets of explosives and collision of plates with obstacles made of St.3 steel, with measurement of the thickness and $\overline{w}$ for the fragments. The sheet charge in contact with the obstacle was detonated in such a way that a load traveling with the detonation speed was generated. We used cast Trotyl + Hexogen 50/50. The charges were made as plates 80 × 150 mm² and of thickness 3 and 5 mm. The colliding plates were made of steel of thickness 1.06 and 1.52 mm and moving at speeds of 0.96 and 0.65 km/sec, respectively. These plates were accelerated by sheet charges. The speeds were measured in separate experiments by electrical-contact and optical methods. The obstacles were

Chelyabinsk. Translated from Zhurnal Prikladnoi Mekhaniki i Tekhnicheskoi Fiziki, No. 1, pp. 151-155, January-February, 1977. Original article submitted February 7, 1976.